PHYSICAL REVIEW D **81,** 054030 (2010)

Inclusive J/ψ production in Υ decay via color-singlet mechanism

Zhi-Guo He[1,2] and Jian-Xiong Wang[1]

[1]*Institute of High Energy Physics, Chinese Academy of Science, P.O. Box 918(4), Beijing, 100049, China, and Theoretical Physics Center for Science Facilities, (CAS) Beijing, 100049, China*

[2]*Departament d'Estructura i Constituents de la Matèria and Institut de Ciències del Cosmos, Universitat de Barcelona, Diagonal, 647, E-08028 Barcelona, Catalonia, Spain*

(Received 1 November 2009; published 30 March 2010)

In this work, we have calculated the tree level color-singlet contribution to the inclusive J/ψ production in Υ decay of the α_s^5 order QCD process $\Upsilon \to J/\psi + c\bar{c}g$ and $\alpha^2\alpha_s^2$ order QED processes $\Upsilon \to \gamma^* \to J/\psi + c\bar{c}$ and $\Upsilon \to J/\psi + gg$. It is found that the contribution of the QED processes is comparable with that of the QCD process and the numerical results of the QCD process alone are about an order of magnitude smaller than the previous theoretical predictions. Our prediction in total is 4.2×10^{-5} which is about an order of magnitude smaller than the recent CLEO measurement on the branching fraction $\mathcal{B}(\Upsilon \to J/\psi + X)$. It indicates that the J/ψ production mechanism in Υ decay is not well understood and further theoretical work and experimental analysis are still necessary.

DOI: 10.1103/PhysRevD.81.054030 PACS numbers: 12.38.Bx, 12.39.Jh, 13.20.Gd

I. INTRODUCTION

Since the discovery of $c\bar{c}$ state J/ψ and $b\bar{b}$ state Υ more than three decades ago, the heavy-quarkonium system has served as a good laboratory for testing QCD from both perturbative and nonperturbative aspects. With the accumulation of new experimental data and the interesting progress in the related theory, considerable attention has been attracted to study heavy-quarkonium spectrum, decay, and production (for a review see [1]).

On the theoretical side, the nonrelativistic QCD (NRQCD) [2] effective field theory was introduced, based on which the production and decay of heavy quarkonium can be calculated with a rigorous factorization formalism. This formalism separates the physics on the energy scale larger than the quark mass m_Q, which is related to the annihilation or production of the $Q\bar{Q}$ pair, from the physics on the scale of $m_Q v^2$ order, which is relevant to the formation of the bound state. Consequently, the inclusive production and decay rates of heavy quarkonium are factorized into the product of the short-distance coefficients, which could be calculated perturbatively through the expansion of α_s, and the corresponding long-distance matrix elements, which can be determined by some nonperturbative methods. The orders of magnitude for the long-distance matrix elements are accounted by the powers of v, the velocity of heavy quark in the rest frame of the bound state. One important feature of NRQCD is that it allows the contribution of the $Q\bar{Q}$ pair in color-octet configuration.

The introduction of NRQCD has greatly improved our understanding of the production mechanism for the heavy quarkonium. One remarkable success of NRQCD is that the transverse momentum (p_t) distributions of J/ψ and ψ' production at Fermilab Tevatron [3] could be well described by the color-octet mechanism [4]. However, this mechanism could not explain the CDF measurements of J/ψ polarization [5]. Recently, the next-to-leading order (NLO) QCD corrections to both the color-singlet and color-octet processes have been obtained. For the color-octet process [6], it is found that the leading-order (LO) results are slightly changed when the NLO QCD corrections are taken into account. In the color-singlet case, the NLO QCD corrections change the LO results of the p_t distribution and polarization distribution significantly [7], although it could not resolve the puzzle. The large impact of NLO QCD corrections on the LO results for the color-singlet process indicates that the contribution of the color-octet mechanism may not be as important as we expected before. Furthermore, the theoretical predictions [8] for the p_t distribution of Υ production can be comparable with the data at Tevatron [9] within the theoretical uncertainty when considering some of the important next-to-next-to-leading-order α_s^5 contribution. However, it still cannot explain the recent polarization measurement by the D0 collaboration [10]

In the case of J/ψ production in e^+e^- annihilation, the existence of the color-octet mechanism also faces a challenge. The NRQCD approach predicts that the J/ψ production in e^+e^- annihilation at LO in α_s is dominated by $e^+e^- \to J/\psi + gg$, $e^+e^- \to J/\psi + c\bar{c}$, and $e^+e^- \to J/\psi + g$, in which the first two are color-singlet subprocesses and the last one is a color-octet subprocess. The color-octet subprocess [11] predicts there is a peak in J/ψ momentum spectrum near the kinematic end point. Unfortunately, the peak was not found in the experimental observation of *BABAR* [12] and Belle [13]. By using the soft-collinear effective theory (SCET), the color-octet predictions [14] could be softened, but it depends on a unknown nonperturbative shape function. Belle also extended their analysis by deriving the associated J/ψ production with the $c\bar{c}$ pair from inclusive J/ψ production [15]. The

NLO QCD calculations show that both $\sigma[e^+e^- \to J/\psi + c\bar{c} + X]$ [16,17] and $\sigma[e^+e^- \to J/\psi + X_{\text{non-}c\bar{c}}]$ [18,19] may be explained by considering only the contribution of color-singlet processes. However, it is pointed out in Ref. [17] that the color-octet contribution is still not yet completely ruled out due to the incomplete measurement in the experimental analysis.

To improve our understanding of the J/ψ production mechanism, it was proposed [20,21] that the J/ψ production in Υ decay may provide an alternate probe to study the J/ψ production mechanism in the rich gluon environment. Experimentally, the branching ratio of $\Upsilon \to J/\psi + X$ was reported to be $(1.1 \pm 0.4 \pm 0.2) \times 10^{-3}$ by the CLEO collaboration [22] based on an analysis of about 20 events. The ARGUS collaboration obtained an upper limit of 0.68×10^{-3} [23] at the 90% confidence level. With about a 35 times larger data sample than the previous work, an improved measurement of the J/ψ branching ratio and momentum spectrum were obtained recently by the CLEO collaboration with $\mathcal{B}(\Upsilon \to J/\psi + X) = (6.4 \pm 0.4 \pm 0.6) \times 10^{-4}$ [24]. Theoretically, the color-octet prediction is $\mathcal{B}(\Upsilon \to J/\psi + X) \simeq 6.2 \times 10^{-4}$ [21] with a 10% contribution from $\psi(2S)$ feed-down and another 10% from χ_{cJ} [25]. However, it was found that the branching ratio of the color-singlet process $\Upsilon \to J/\psi + c\bar{c}g$ is about 5.9×10^{-4} [26], which is also in agreement with experimental measurement. Although both the color-singlet and color-octet decay modes can explain the total decay rate independently, their predictions on the J/ψ momentum spectrum are significantly different. The maximum value of J/ψ momentum in the color-singlet and color-octet processes are 3.7 and 4.5 GeV, respectively. The results of CLEO show that the J/ψ momentum spectrum is much softer than the color-octet prediction and somewhat softer than the color-singlet prediction. The process $\Upsilon \to J/\psi + X$ was also studied in the color evaporation model [27] more than 30 years ago, but this model cannot give systematic predictions of J/ψ production. Another early theoretical work on the process $\Upsilon \to J/\psi + X$ could be found in Ref. [28].

There is a very good agreement between the LO color-singlet predictions [26] and experimental measurements [24]. But it seems difficult to understand the situation in comparison with the case of the J/ψ production at B factories, where there are huge discrepancies between the LO theoretical predictions and the experimental measurements. Therefore, we recalculate the branching ratio of the color-singlet process $\Upsilon \to J/\psi + c\bar{c}g$ in this paper. The obtained result is an order of magnitude smaller than the prediction given in Ref. [26]. We have confirmed our results by doing two completely independent calculations. One is to do all the calculations by writing a piece of program in MATHEMATICA with the help of the FEYNCALC package. The other is to use the Feynman diagram calculation (FDC) Package [29] to generate all the needed FORTRAN source and do the numerical calculation. We obtained exactly the same results. Moreover, to check gauge invariance, the gluon polarization vector is explicitly kept and then is replaced by its 4-momentum in the final numerical calculation in the FDC version source. Definitely, the result must be zero and our result confirms it. Then we had a detailed discussion with Dr. Li, one of the authors of the previous prediction [26], and found that there is an error in the color factor treatment in their calculation.

Therefore, the correct α_s^5 color-singlet prediction cannot explain the CLEO experimental measurement for $\Upsilon \to J/\psi + X$ now and more theoretical consideration are needed. So we further estimate the leading-order contributions of the QED processes $\Upsilon \to \gamma^* \to J/\psi + c\bar{c}$ and $\Upsilon \to J/\psi + gg$ at $\alpha^2\alpha_s^2$ order, in which the process $\Upsilon \to J/\psi + gg$ includes two gauge invariant subsets, $\Upsilon \to \gamma^* \to J/\psi + gg$ and $\Upsilon \to \gamma^* gg$ followed by $\gamma^* \to J/\psi$. The final results show that the contributions of the QED processes are comparable with that from the QCD process.

The rest of the paper is organized as follows: In Sec. II, we describe the calculation on the branching ratio and J/ψ momentum spectrum of the QCD process $\Upsilon \to J/\psi + c\bar{c}g$. In Sec. III, we estimate the contribution of the two QED processes $\Upsilon \to J/\psi + c\bar{c}$ and $\Upsilon \to J/\psi + gg$. The final results and summary are given in the last section. In Appendix A, the basic formula and method used in the calculation are presented. A detailed treatment of the four-body phase space is given in Appendix B.

II. THE QCD PROCESS $\Upsilon \to J/\psi + c\bar{c}g$

Now we proceed to calculate the total decay rate of $\Upsilon \to J/\psi + c\bar{c}g$ and its contribution to the J/ψ momentum spectrum. At leading order in α_s, there are six Feynman diagrams shown in Fig. 1. The amplitude $\mathcal{M}$ could be factorized as

$$\begin{aligned}\mathcal{M}(b\bar{b}[^3S_1, \underline{1}](p_0) \to c\bar{c}[^3S_1, \underline{1}](p_1) + c(p_2)\bar{c}(p_3) \\ + g(p_4)) \\ = \mathcal{M}_b(b\bar{b}[^3S_1, \underline{1}] \\ \to g^*g^*g) \times \mathcal{M}_c(g^*g^* \\ \to c\bar{c}[^3S_1, \underline{1}] + c\bar{c}),\end{aligned} \tag{1}$$

in which the later one is universal for all six diagrams and it is

$$\mathcal{M}_c = \frac{g_s^2}{(p_2 + p_1/2)^2(p_3 + p_1/2)^2}\bar{u}(p_2)\gamma^\mu \Pi_c \gamma^\nu v(p_3). \tag{2}$$

The amplitude of $\mathcal{M}_b(b\bar{b}[^3S_1, \underline{1}] \to g^*g^*g)$, for example, for the first diagram is

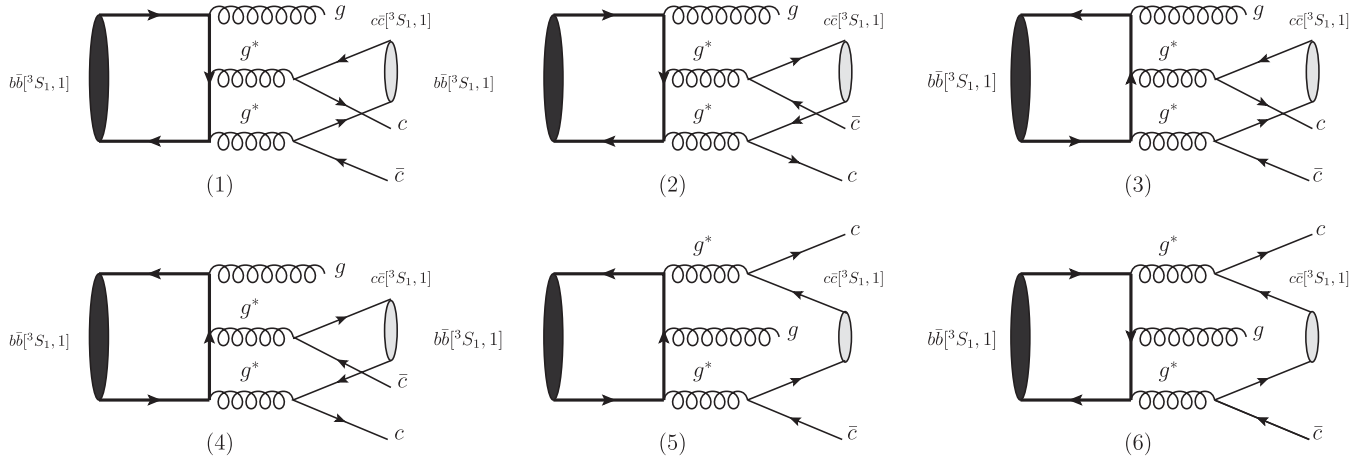

FIG. 1. The six Feynman diagrams for the short-distance process: $b\bar{b}[^3S_1, 1] \to c\bar{c}[^3S_1, 1] + c\bar{c}g$.

$$\mathcal{M}_b^1 = g_s^3 C_1 \,\mathrm{Tr}\Big[\Pi_b \gamma^\mu \frac{\frac{-\not{p}_0}{2} + \frac{\not{p}_1}{2} + \not{p}_3 + m_b}{(-p_0/2 + p_1/2 + p_3)^2 - m_b^2} \times \gamma^\nu \frac{\frac{\not{p}_0}{2} - \not{p}_4 + m_b}{(p_0/2 - p_4)^2 - m_b^2} \not{\epsilon}_3\Big], \tag{3}$$

where Π_c and Π_b are the projection operators defined in Appendix A, C_1 is the corresponding color coefficient, and $\not{\epsilon}_3$ is the polarization vector of the real gluon. The amplitude $\mathcal{M}_b^i$ for the other five diagrams could be obtained in a similar way. An analytical expression of $\sum |\mathcal{M}|^2$ is obtained in the calculation, but is too lengthy to be presented here.

By dimension analysis, it is easy to represent the decay width and differential decay width of $\Upsilon \to J/\psi + c\bar{c}g$ as

$$\Gamma(\Upsilon \to J/\psi + c\bar{c}g) = \frac{\alpha_s^5}{m_b^5} f(r) \frac{\langle \Upsilon|\mathcal{O}_1(^3S_1)|\Upsilon\rangle}{2N_c} \times \frac{\langle \mathcal{O}_1^\psi(^3S_1)\rangle}{3 \times 2N_c}, \tag{4a}$$

$$\frac{d\Gamma}{d|\vec{p}_1|}(\Upsilon \to J/\psi + c\bar{c}g) = \frac{\alpha_5^s}{m_b^6} g(r, |\vec{p}_1|/m_b) \frac{\langle \Upsilon|\mathcal{O}_1(^3S_1)|\Upsilon\rangle}{2N_c} \times \frac{\langle \mathcal{O}_1^\psi(^3S_1)\rangle}{3 \times 2N_c}, \tag{4b}$$

where $r = m_c/m_b$ and $f(r)$ are dimensionless, and the function $f(r)$ is the same as $h(r)$ in Ref. [26]. To ensure the validity of our calculations, we use two different kinds of computer codes for cross-check and obtain exactly the same results for $f(r)$ and $g(r, |\vec{p}_1|/m_b)$. When $r = \frac{1.548}{4.73} = 0.327$, the decay width is

$$\Gamma(\Upsilon \to J/\psi + c\bar{c}g) = \frac{\alpha_s^5}{m_b^5} \frac{\langle \Upsilon|\mathcal{O}_1(^3S_1)|\Upsilon\rangle}{2N_c} \frac{\langle \mathcal{O}_1^\psi(^3S_1)\rangle}{3 \times 2N_c} \times 0.269. \tag{5}$$

Our results of $f(r)$ in the range $0.275 < r < 0.381$ are listed in Table I. They are about an order of magnitude smaller than those given in Ref. [26]. The range of r is obtained by fixing $m_b = M_\Upsilon/2 = 4.73$ GeV and varying m_c from 1.3 to 1.8 GeV. In addition to $f(r)$, the decay width $\Gamma(\Upsilon \to J/\psi + c\bar{c}g)$ is also dependent on the choice of the values of the two long-distance matrix elements $\langle \Upsilon|\mathcal{O}_1(^3S_1)|\Upsilon\rangle$, $\langle \mathcal{O}_1^\psi(^3S_1)\rangle$, the mass of c and b quark, particularly on the coupling constant α_s, for it is an α_s^5 order process. Since the process $\Upsilon \to J/\psi + c\bar{c}g$ can be viewed as $\Upsilon \to gg^*g^*$ followed by $g^*g^* \to J/\psi + c\bar{c}$, the α_s and m_b dependence of our theoretical result can be reduced if we normalize it by the theoretical prediction on the decay width of $\Upsilon \to$ light hadron, which includes the dominant decay modes $\Upsilon \to ggg$ staring at α_s^3 order and $\Upsilon \to \gamma^* \to q\bar{q}$ ($q = u, d, s, c$) starting at α^2 order. In the nonrelativistic limit, the tree level results for Υ decays into $3g$ and $q\bar{q}$ are given by

$$\Gamma(\Upsilon \to ggg) = \frac{20\alpha_s^3(\pi^2 - 9)}{243 m_b^2} \langle \Upsilon|\mathcal{O}_1(^3S_1)|\Upsilon\rangle, \tag{6a}$$

$$\Gamma(\Upsilon \to q\bar{q}) = \frac{2\pi N_c e_q^2 e_b^2 \alpha^2}{3 m_b^2} \langle \Upsilon|\mathcal{O}_1(^3S_1)|\Upsilon\rangle. \tag{6b}$$

Then the normalized width $\Gamma_{\mathrm{nor}}^{c\bar{c}g}$ is given by

$$\Gamma_{\mathrm{nor}}^{c\bar{c}g} = \frac{f(r)\alpha_s^5 \langle \mathcal{O}_1^\psi(^3S_1)\rangle}{3(2N_c)^2(\frac{20}{243}\alpha_s^3(\pi^2 - 9) + \sum_q \frac{2}{3}\pi N_c e_q^2 e_b^2 \alpha^2) m_b^3}. \tag{7}$$

Since the $3g$ process is dominant in Υ decay, the normalized width $\Gamma_{\mathrm{nor}}^{c\bar{c}g}$ will only be proportional to α_s^2 approximately. The branching ratio then can be estimated by

$$\mathcal{B}(\Upsilon \to J/\psi + c\bar{c}g) = \Gamma_{\mathrm{nor}}^{c\bar{c}g} \times \mathcal{B}(\Upsilon \to \text{light hadron}). \tag{8}$$

TABLE I. The values of $f(r)$ for different $r = m_c/m_b$.

r	0.275	0.296	0.317	0.327	0.338	0.361	0.381
$f(r)$	0.904	0.567	0.345	0.269	0.202	0.105	0.055

There are two typical scales m_b and m_c in this process. Since the $\Upsilon \to J/\psi + c\bar{c}g$ process can be divided into $\Upsilon \to gg^*g^*$ and $g^*g^* \to J/\psi + c\bar{c}$, the m_b scale dependence of process $\Upsilon \to gg^*g^*$ is canceled partly in Eq. (7) although not entirely. Then we choose the scale to be $2m_c$ but not $2m_b$ in a similar way as that suggested in Ref. [20]. Setting $e_u = e_c = \frac{2}{3}$, $e_d = e_s = e_b = -\frac{1}{3}$, $\alpha = \frac{1}{128}$, $r = \frac{1.548}{4.73} \simeq 0.327$, $m_b = 4.73$ GeV, $|R_\psi(0)|^2 = 0.81$ GeV^3 being calculated in potential model [30], $\mathcal{B}(\Upsilon \to \text{light hadron}) = 92\%$ [31], and $\alpha_s(2m_c) = 0.259$, we predict

$$\mathcal{B}(\Upsilon \to J/\psi + c\bar{c}g) = 2.27 \times 10^{-5}. \tag{9}$$

The normalized J/ψ momentum spectrum $d\Gamma_{\text{nor}}/d|\vec{p}_1|$ is shown in Fig. 3. It is easy to see that the shape of the J/ψ momentum spectrum is similar to that in Ref. [26], although the prediction for the total decay width is an order of magnitude smaller than the experimental data.

III. THE QED PROCESS $\Upsilon \to J/\psi + X$

There are two QED processes $\Upsilon \to J/\psi + c\bar{c}$ and $\Upsilon \to J/\psi + gg$ at the leading order in α_s and α. Both of them are considered in this work and the analytical results will be presented in the following.

A. $\Upsilon \to \gamma^* \to J/\psi + c\bar{c}$

At the leading order, there are four Feynman diagrams for $\Upsilon(p_0) \to \gamma^* \to J/\psi(p_1) + c(p_2)\bar{c}(p_3)$, two of which are shown in Fig. 2(a). The calculation procedure for this process is very similar to that for the J/ψ production in association with the $c\bar{c}$ pair in e^+e^- annihilation. The differential decay width is given by

$$\begin{aligned}
&\frac{d\Gamma}{d|\vec{p}_1|}(\Upsilon \to \gamma^* \to J/\psi + c\bar{c}) \\
&= \frac{2\pi C_A C_F^2 e_b^2 e_c^2 \alpha^2 \alpha_s^2 \langle \Upsilon|\mathcal{O}_1(^3S_1)|\Upsilon\rangle\langle \mathcal{O}_1^\psi(^3S_1)\rangle\sqrt{x_1^2 - 4r^2}}{9(2N_c)^2 m_b^6 r x_1^4(\kappa - x_1)^3(-2 + x_1)^2(\kappa + x_1)^3}\Big(-2\kappa x_1((-6x_1^6 + 8\kappa^2 x_1^4 - 24x_1^4 + 64\kappa^2 x_1^3 - 18\kappa^4 x_1^2 \\
&- 64\kappa^2 x_1^2 + 24\kappa^4)r^6 + (-4x_1^7 + 104x_1^6 - 32\kappa^2 x_1^5 - 128x_1^5 - 104\kappa^2 x_1^4 - 32x_1^4 + 36\kappa^4 x_1^3 + 320\kappa^2 x_1^3 - 32\kappa^4 x_1^2 \\
&- 160\kappa^2 x_1^2 - 64\kappa^4 x_1 + 64\kappa^4)r^4 + (-39x_1^8 + 60x_1^7 + 74\kappa^2 x_1^6 + 124x_1^6 - 152\kappa^2 x_1^5 - 128x_1^5 - 39\kappa^4 x_1^4 - 120\kappa^2 x_1^4 \\
&+ 32x_1^4 + 92\kappa^4 x_1^3 + 192\kappa^2 x_1^3 + 4\kappa^6 x_1^2 - 4\kappa^4 x_1^2 - 64\kappa^2 x_1^2 - 64\kappa^4 x_1 + 32\kappa^4)r^2 + (-18x_1^9 + 8x_1^8 + 36\kappa^2 x_1^7 \\
&- 14\kappa^2 x_1^6 + 8x_1^6 - 18\kappa^4 x_1^5 + 4\kappa^4 x_1^4 - 16\kappa^2 x_1^4 + 2\kappa^6 x_1^2 + 8\kappa^4 x_1^2)) - (\kappa^2 - x_1^2)^3(6(x_1^2 + 4)r^6 - 4(5x_1^3 - 4x_1^2 \\
&+ 16x_1 - 16)r^4 - (-7x_1^4 + 4x_1^3 + 4x_1^2 + 64x_1 - 32)r^2 - 2x_1^2(8x_1^3 - 13x_1^2 + 4))\log\frac{x_1 - \kappa}{x_1 + \kappa}\Big),
\end{aligned} \tag{10}$$

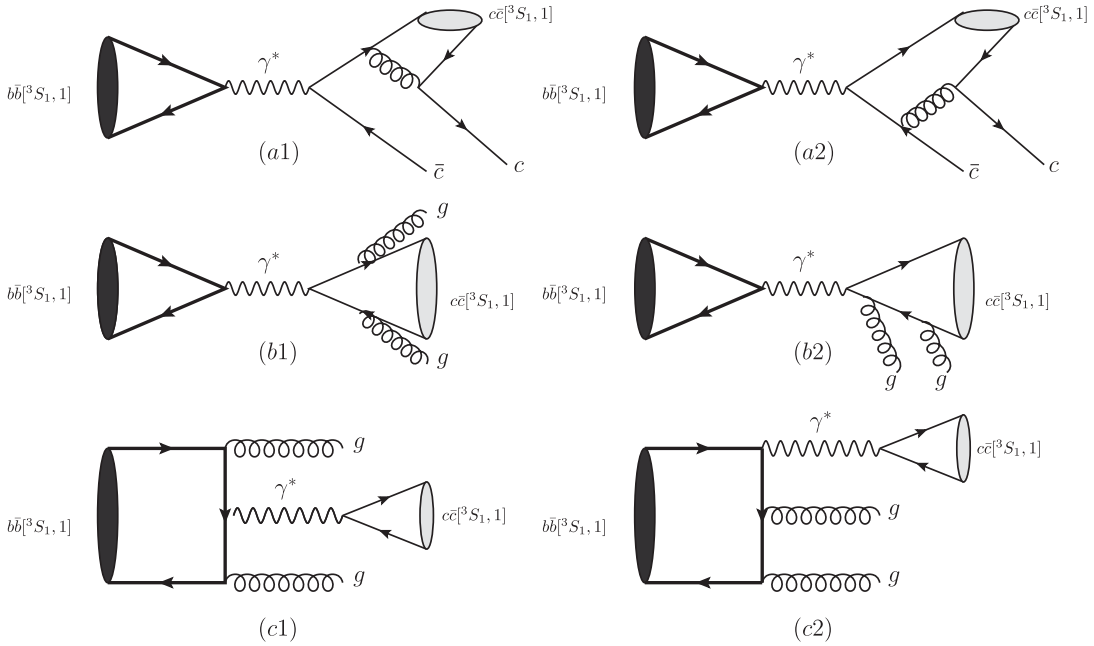

FIG. 2. The typical Feynman diagrams for the QED processes of inclusive J/ψ production: (a) $b\bar{b}[^3S_1, 1] \to \gamma^* \to c\bar{c}[^3S_1, 1] + c\bar{c}$, (b) $b\bar{b}[^3S_1, 1] \to \gamma^* \to c\bar{c}[^3S_1, 1] + gg$, and (c) $b\bar{b}[^3S_1, 1] \to c\bar{c}[^3S_1, 1] + gg$.

where $C_A = 3$ and $C_F = \frac{4}{3}$ are the color factors, $x_1 = \sqrt{|\vec{p}_1|^2 + 4m_c^2}/m_b$ and $\kappa = \sqrt{(x_1 + 2r)(x_1 - 2r)(1 + r^2 - x_1)(1 - x_1)}/(1 + r^2 - x_1)$.

Integrating $|\vec{p}_1|$ numerically and normalizing $\Gamma(\Upsilon \to \gamma^* \to J/\psi + c\bar{c})$ by $\Gamma(\Upsilon \to \text{light hadron})$, we obtain

$$\Gamma^{c\bar{c}}_{\text{normal}} = \frac{\Gamma(\Upsilon \to \gamma^* \to J/\psi + c\bar{c})}{\Gamma(\Upsilon \to \text{light hadron})} = \frac{3.85\alpha^2\alpha_s^2\langle \mathcal{O}_1^{\psi}(^3S_1)\rangle}{6N_c(\frac{20}{243}\alpha_s^3(\pi^2 - 9) + \sum_q \frac{2}{3}\pi e_q^2 e_b^2 \alpha^2)m_b^3}. \quad (11)$$

By choosing the same numerical values for r, m_b, e_q, α, $\langle \mathcal{O}_1^{\psi}(^3S_1)\rangle$, and $\mathcal{B}(\Upsilon \to \text{light hadron})$ as those in Sec. III, the numerical result is

$$\mathcal{B}(\Upsilon \to \gamma^* \to J/\psi + c\bar{c}) = 1.14 \times 10^{-6}, \quad (12)$$

and the normalized J/ψ momentum spectrum is shown in Fig. 3.

B. $\Upsilon \to J/\psi + gg$

The process $\Upsilon(p_0) \to J/\psi(p_1) + g(p_2)g(p_3)$ includes two parts, $\Upsilon \to \gamma^* \to J/\psi + gg$ and $\Upsilon \to gg\gamma^*$ ($\gamma^* \to J/\psi$). There are six Feynman diagrams for each part at the leading order and the typical ones are shown in Figs. 2(b) and 2(c). We calculate the contribution of the two parts together and the differential decay width is expressed as

$$\begin{aligned}
&\frac{d\Gamma}{d|\vec{p}_1|}(\Upsilon \to J/\psi + gg) \\
&= \frac{32\pi C_A C_F e_c^2 e_b^2 \alpha^2 \alpha_s^2 \langle \Upsilon|\mathcal{O}_1(^3S_1)|\Upsilon\rangle\langle \mathcal{O}_1^{\psi}(^3S_1)\rangle\sqrt{x_1^2 - 4r^2}}{9(2N_c)^2 m_b^6 r^3 x_1(-1 + r^2)(2r^2 - x_1)^3(-2 + x_1)^3}\Big((r^2 - 1)(2r^2 - x_1)(-2 + x_1)\sqrt{-4r^2 + x_1^2} \\
&\times (8r^8 - 4(3x_1 - 4)r^6 + (7x_1^2 - 30x_1 + 32)r^4 - 2(x_1^3 - 8x_1^2 + 15x_1 - 8)r^2 - 2x_1^3 + 7x_1^2 - 12x_1 + 8) \\
&+ 2(1 + r^2 - x_1)\Big((x_1 - 2r^2)(2r^8 + (5x_1^2 - 32x_1 + 40)r^6 + (-6x_1^3 + 31x_1^2 - 38x_1 + 6)r^4 \\
&+ x_1(2x_1^3 - 10x_1^2 + 13x_1 - 6)r^2 + 5x_1^2 - 12x_1 + 8)\log\Big(\frac{-2 + x_1 - \sqrt{-4r^2 + x_1^2}}{-2 + x_1 + \sqrt{-4r^2 + x_1^2}}\Big) + 2r^2(-2 + x_1)(8r^{10} - 12x_1 r^8 \\
&+ (5x_1^2 - 6x_1 + 6)r^6 + (13x_1^2 - 38x_1 + 40)r^4 + (-10x_1^3 + 31x_1^2 - 32x_1 + 2)r^2 + x_1^2(2x_1^2 - 6x_1 + 5)) \\
&\times \log\Big(\frac{-2r^2 + x_1 + \sqrt{-4r^2 + x_1^2}}{-2r^2 + x_1 - \sqrt{-4r^2 + x_1^2}}\Big)\Big)\Big), \quad (13)
\end{aligned}$$

where $x_1 = \sqrt{|\vec{p}_1|^2 + 4m_c^2}/m_b$, and the normalized decay width becomes

$$\Gamma^{gg}_{\text{Normal}} = \frac{\Gamma(\Upsilon \to J/\psi + gg)}{\Gamma(\Upsilon \to \text{light hadron})} = \frac{60.8\alpha^2\alpha_s^2\langle \mathcal{O}_1^{\psi}(^3S_1)\rangle}{6N_c(\frac{20}{243}\alpha_s^3(\pi^2 - 9) + \sum_q \frac{2}{3}\pi e_q^2 e_b^2 \alpha^2)m_b^3}. \quad (14)$$

By using the same parameters as above, we obtain

$$\mathcal{B}(\Upsilon \to J/\psi + gg) = 1.79 \times 10^{-5} \quad (15)$$

and the normalized J/ψ momentum spectrum is plotted in Fig. 3. In the numerical result, about 85.2% contribution comes from the $\Upsilon \to gg\gamma^*(J/\psi)$ part, 18.2% from the $\Upsilon \to \gamma^* \to J/\psi gg$ part, and -3.4% from the interference part.

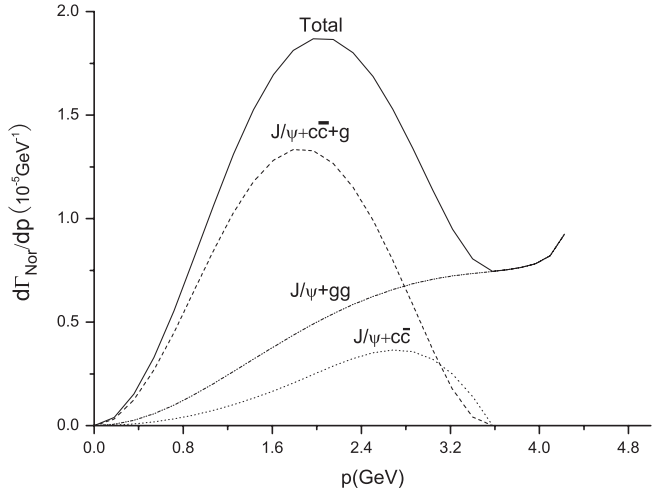

FIG. 3. The contributions of the QCD process $\Upsilon \to J/\psi + c\bar{c}g$ (dashed line) and QED processes $\Upsilon \to J/\psi + gg$ (dot-dashed line) and 5 times of $\Upsilon \to \gamma^* \to J/\psi + c\bar{c}$ (dotted line) to J/ψ momentum distribution for J/ψ production in Υ decay. The sum of them is given by the solid line.

IV. SUMMARY AND DISCUSSION

Summing up all the contributions of the color-singlet QED and QCD processes considered above, we predict that

the branching ratio of direct J/ψ production in Υ decay is

$$\mathcal{B}_{\text{direct}}(\Upsilon \to J/\psi + X) = 4.2 \times 10^{-5}. \quad (16)$$

The corresponding normalized J/ψ momentum distribution is given by the solid line in Fig. 3. It can be seen in Fig. 3 that the contribution of the QCD process is dominated in the small p_ψ region, while the effect of the QED process $J/\psi + gg$ is more important in the large p_ψ region. In Eq. (13) and the dot-dashed line in Fig. 3, the logarithmic divergence at the kinematic end point is obviously shown for the QED process $J/\psi + gg$. It was pointed out in Refs. [14,18,32] that both the α_s and v_b expansion failed near the kinematic end point region in the similar processes $e^+e^- \to J/\psi + X$ and $\Upsilon \to \gamma + X$ because of the large perturbative and nonperturbative corrections, and the logarithmic divergent behavior can be softened by applying the resummation in the SCET. It can improve the J/ψ momentum spectrum largely near the kinematic end point, but the correction for the total decay width is small. Therefore we omit the resummation effect here.

Our calculations show that at the leading order in α_s, v_b, and v_c, the QCD process $\Upsilon \to J/\psi + c\bar{c}g$ only accounts for 54.4% of the LO theoretical prediction for total branching ratio in spite of an enhancement factor α_s^3/α^2 of the coupling constants comparing to the QED processes. The main reasons are that the virtuality of the two virtual gluons are both of m_b^2 order in the QCD process while the virtuality of the photon is fixed to $4m_c^2$ in the QED processes dominated by $\Upsilon \to gg\gamma^*(J/\psi)$ and also the four-body phase space of the QCD process is smaller than the three-body one of the QED processes.

On the experimental side, the CLEO collaboration finds [24] that the feed-down of χ_{cJ} to J/ψ is $<8.2\%$, 11%, 10% for $J = 0, 1, 2$, respectively, and the feed-down of $\psi(2S)$ is about 24% in $\Upsilon \to J/\psi + X$. So the center value of the experimental result for the direct J/ψ production is

$$\mathcal{B}_{\text{Direct}}(\Upsilon \to J/\psi + X) = 3.52 \times 10^{-4} \quad (17)$$

which is about 8.4 times larger than our results. This means that, unlike the conclusion before [26], the branching ratio of $\Upsilon \to J/\psi + X$ cannot be explained by the color-singlet model at the leading order.

The theoretical predication from the color-octet mechanism can account for most J/ψ production in Υ decay, but its prediction for the J/ψ momentum spectrum is not in agreement with the experimental data. The renewed color-singlet prediction for the shape of the J/ψ momentum spectrum is closer to the experimental result, but the discrepancy of the branching ratio between them is large. For all the numerical results above, we used the theoretically normalized decay width to estimate the branching ratios. If we calculate the partial decay width directly with the input of $\langle \Upsilon | O_1(^3S_1) | \Upsilon \rangle = 2.9\ \text{GeV}^3$ [20] and divide it by the total decay width $\Gamma_\Upsilon = 51.4$ keV [31], the branching ratio will be enhanced by a factor of about 3, which still cannot explain the experimental results. Furthermore, as we discussed in Sec. III, the numerical prediction quite strongly depends on the scale choice of α_s, and the branching ratio given in Eq. (16) corresponds to $\alpha_s(2m_c) = 0.259$. If we chose the scale to be $2m_b$ and $2\sqrt{m_b m_c}$, the theoretical predictions become 3.6×10^{-5} and 3.7×10^{-5}, respectively, which become even smaller. It indicates that the NLO QCD correction should be important if the color-singlet mechanism can explain the experimental data just like in the known cases. For example, the NLO QCD corrections for J/ψ production in e^+e^- annihilation show that the K factors are about 1.97 and 1.2 for $e^+e^- \to \gamma^* \to J/\psi + c\bar{c}$ and $e^+e^- \to \gamma^* \to J/\psi + gg$ processes, respectively, and the NLO QCD corrections to $\eta_b \to J/\psi J/\psi$ and $\Upsilon \to J/\psi + \eta_c$ are also found to be quite important [33]. In addition, the contribution of $\mathcal{O}(\alpha_s^6)$ processes $b\bar{b}(^3S_1, 1) \to c\bar{c}(^3S_1, 1) + gg$ and $b\bar{b}(^3S_1, 1) \to c\bar{c}(^3S_1, 1) + gggg$ to the branching ratio has been estimated to be of 10^{-4} order [25]. So that the next important step is to give an explicit and complete calculation of them, which will be very helpful to understand the conflict between the color-singlet prediction and the CLEO result [24]. Furthermore, to obtain the full QCD correction for the inclusive J/ψ production in Υ decay would be very interesting and challenging work, to explain the experimental data. But it will involve very complicated work at the QCD NLO and is beyond the scope of this paper.

ACKNOWLEDGMENTS

We thank Dr. S. Y. Li for helpful discussions. This work was supported by the National Natural Science Foundation of China (No. 10775141), Chinese Academy of Sciences under Project No. KJCX3-SYW-N2, and in part by the Project of Knowledge Innovation Program (PKIP) of Chinese Academy of Sciences, Grant No. KJCX2.YW.W10. Zhiguo He is currently supported by the CPAN08-PD14 contract of the CSD2007-00042 Consolider-Ingenio 2010 program, and by the FPA2007-66665-C02-01/ project (Spain).

APPENDIX A: DESCRIPTION OF OUR BASIC CALCULATION FORMULA

At leading order in v_Q, for S-wave heavy-quarkonium production and decay, the color-singlet model predictions are equal to that based on NRQCD effective theory. Then we express $d\Gamma(\Upsilon \to J/\psi + X)$ as

$$d\Gamma(\Upsilon \to J/\psi + X) = d\hat{\Gamma}(b\bar{b}[^3S_1, \underline{1}] \to c\bar{c}[^3S_1, \underline{1}] + X) \langle \Upsilon | \mathcal{O}_1(^3S_1) | \Upsilon \rangle \langle \mathcal{O}_1^{\psi}(^3S_1) \rangle, \quad (A1)$$

where $d\Gamma(b\bar{b}[^3S_1, \underline{1}] \to c\bar{c}[^3S_1, \underline{1}] + X)$ represents the color-singlet $b\bar{b}$ pair in the spin-triplet state decay into a color-singlet $c\bar{c}$ pair in a spin-triplet state plus anything, which is calculated perturbatively, and $\langle \Upsilon | \mathcal{O}_1(^3S_1) | \Upsilon \rangle$ and

$\langle \mathcal{O}_1^{\psi}(^3S_1)\rangle$ are the long-distance matrix elements, which can be related to the nonrelativistic wave functions as

$$\langle \Upsilon|\mathcal{O}_1(^3S_1)|\Upsilon\rangle \simeq \frac{3}{2\pi}|R_\Upsilon(0)|^2,$$
$$\langle \mathcal{O}_1^{\psi}(^3S_1)\rangle \simeq \frac{9}{2\pi}|R_\psi(0)|^2. \tag{A2}$$

We employ the spinor projection method [34] to calculate the short-distance part $d\hat{\Gamma}$. In the nonrelativistic limit, the amplitude of $b\bar{b}[^3S_1, \underline{1}] \to c\bar{c}[^3S_1, \underline{1}] + X$ could be written as [35]

$$\begin{aligned}\mathcal{M}(b\bar{b}[^3S_1, \underline{1}](p_0) \to c\bar{c}[^3S, \underline{1}](p_1) + X) &= \sum_{s_1,s_2}\sum_{i,l}\sum_{s_3,s_4}\sum_{k,l}\langle s_1; s_2 \mid 1S_z\rangle \\ &\times \langle 3i; \bar{3}j \mid 1\rangle \times \langle s_3; s_4 \mid 1S_z'\rangle \\ &\times \langle 3k; \bar{3}l \mid 1\rangle \\ \mathcal{M}\left(b_i\left(\frac{p_0}{2}, s_1\right)\bar{b}_j\left(\frac{p_0}{2}, s_2\right) \to c_k\left(\frac{p_1}{2}, s_3\right)\bar{c}_l\left(\frac{p_1}{2}, s_4\right) + X\right),\end{aligned} \tag{A3}$$

where $\langle 3i; \bar{3}j \mid 1\rangle = \delta_{ij}/\sqrt{N_c}$, $\langle 3k; \bar{3}l \mid 1\rangle = \delta_{kl}/\sqrt{N_c}$, $\langle s_1; s_2 \mid 1S_z\rangle$, and $\langle s_3; s_4 \mid 1S_z'\rangle$ are the SU(3)-color, SU(2)-spin, and angular momentum Clebsch-Gordan coefficients for $Q\bar{Q}$ projecting on certain appropriate configurations at short distance. At leading order in v_Q ($Q = b,\ c$), the projection of spinors $u(\frac{p_0}{2}, s_1)\bar{v}(\frac{p_0}{2}, s_2)$ and $v(\frac{p_1}{2}, s_3)\bar{u}(\frac{p_1}{2}, s_4)$ could be expressed as

$$\begin{aligned}\Pi_b &= \sum_{s_1,s_2}\langle s_1; s_2 \mid 1S_z\rangle u\left(\frac{p_0}{2}, s_1\right)\bar{v}\left(\frac{p_0}{2}, s_2\right) \\ &= \frac{1}{2\sqrt{2}}\not{\epsilon}(S_z)(\not{p}_0 - 2m_b), \qquad \text{(A4a)} \\ \Pi_c &= \sum_{s_3,s_4}\langle s_3; s_4 \mid 1S_z'\rangle v\left(\frac{p_1}{2}, s_3\right)\bar{u}\left(\frac{p_1}{2}, s_4\right) \\ &= \frac{1}{2\sqrt{2}}\not{\epsilon}(S_z')(\not{p}_1 + 2m_c), \qquad \text{(A4b)}\end{aligned}$$

where $\epsilon(S_z)$ and $\epsilon(S_z')$ are the polarization vectors of Υ and J/ψ, respectively. For a spin $= 1$ state with momentum p, the sum over all its possible states S_z is

$$\sum_{S_z}\epsilon_\alpha(S_z)\epsilon_\beta^*(S_z) = \left(-g_{\alpha\beta} + \frac{p_\alpha p_\beta}{p^2}\right). \tag{A5}$$

According to the spinor projection method, the relation between $d\hat{\Gamma}$ and $|\mathcal{M}|^2$ for the $b\bar{b}[^3S_1, \underline{1}] \to c\bar{c}[^3S_1, \underline{1}] + X$ is

$$\begin{aligned}d\hat{\Gamma}(b\bar{b}[^3S_1, \underline{1}] \to c\bar{c}[^3S_1, \underline{1}] + c\bar{c}g) \\ = \frac{1}{3}\frac{1}{4m_b}\frac{\sum|\mathcal{M}|^2}{3m_b m_c(2N_c)^2}d\Phi_n,\end{aligned} \tag{A6}$$

where $\sum$ means to sum over all possible polarization states of the particles in this process and Φ_n is the n-body phase space. The factor $(1/2N_c)^2$ with $N_c = 3$ comes from the normalization factor of the NRQCD four-fermion operator.

APPENDIX B: THE FOUR-BODY PHASE-SPACE TREATMENT

The four-body phase space Φ_4 for $b\bar{b}[^3S_1, \underline{1}] \to c\bar{c}[^3S_1, \underline{1}] + c\bar{c}g$ is defined as

$$d\Phi_4(p_0 \to p_1 + p_2 + p_3 + p_4) = \prod_{k=1}^{4}\frac{d^3\vec{p}_k}{(2\pi)^3 2E_k}(2\pi)^4 \times \delta^4\left(p_0 - \sum_{k=1}^{4}p_k\right). \tag{B1}$$

There are many ways to perform the four-body phase-space integration. Here we briefly introduce our method. Using the two following identical equations,

$$\int\frac{d^4p_{234}}{(2\pi)^4}(2\pi)^4\delta^4(p_{234} - p_2 - p_3 - p_4) \equiv 1,$$
$$\int\frac{d^4p_{34}}{(2\pi)^4}(2\pi)^4\delta^4(p_{34} - p_3 - p_4) \equiv 1, \tag{B2}$$

we transform the four-body space into the combination of three two-body phase spaces, which is given by

$$\begin{aligned}d\Phi_4(p_0 \to p_1 + p_2 + p_3 + p_4) &= \frac{ds_{234}}{2\pi}\frac{ds_{34}}{2\pi} \\ d\Phi_2(p_0 \to p_1 + p_{234})d\Phi_2(p_{234} \to p_2 + p_{34}) &\times d\Phi_2(p_{34} \to p_3 + p_4),\end{aligned} \tag{B3}$$

where $s_{234} = p_{234}^2$, $s_{34} = p_{34}^2$. The three two-body phase space integrations are described by the three-momenta $\vec{p}_1$, $\vec{p}_2^*$, $\vec{p}_3^{**}$ and their solid angle element $d\Omega_0$, $d\Omega_{234}^*$, $d\Omega_{34}^{**}$ in the rest frames of p_0, p_{234}, and p_{34}, respectively. Then the expression of four-body phase space becomes

$$\begin{aligned}d\Phi_4 = \int\frac{ds_{234}}{2\pi}\int\frac{|\vec{p}_1|}{8(2\pi)^2 m_b}d\Omega_0\int\frac{ds_{34}}{2\pi} \\ \times\int d\Omega_{234}^*\frac{|\vec{p}_2^*|}{4(2\pi)^2\sqrt{s_{234}}}\int\frac{|\vec{p}_3^{**}|}{4(2\pi)^2\sqrt{s_{34}}}d\Omega_{34}^{**},\end{aligned} \tag{B4}$$

where $|\vec{p}_1|$, $|\vec{p}_2^*|$, and $|\vec{p}_3^{**}|$ are given in the equations below in the rest frame of p_0, p_{234}, and p_{34}, respectively,

$$|\vec{p}_1| = \frac{\sqrt{16m_b^4 + (-4m_c^2 + s_{234})^2 - 8m_b^2(4m_c^2 + s_{234})}}{4m_b} \tag{B5a}$$

$$|\vec{p}_2^*| = \frac{\sqrt{(s_{234} - (m_c - \sqrt{s_{34}})^2)(s_{234} - (m_c + \sqrt{s_{34}})^2)}}{2\sqrt{s_{234}}} \tag{B5b}$$

$$|\vec{p}_3^{**}| = \frac{s_{34} - m_c^2}{2\sqrt{s_{34}}}. \tag{B5c}$$

The integration ranges of s_{234} and s_{34} are

$$\begin{aligned} 4m_c^2 < s_{234} < (2m_b - 2m_c)^2, \\ m_c^2 < s_{34} < (\sqrt{s_{234}} - m_c)^2. \end{aligned} \tag{B6}$$

For space symmetry, $d\Omega_0$ and $d\phi_{234}^*$ could be integrated out directly and $|\mathcal{M}|^2$ only depends on the five variables s_{234}, s_{34}, θ_{234}^*, θ_{34}^{**}, and ϕ_{34}^{**}. To get the total decay rate, the nontrivial integral with these five variables is performed by three steps. First, we do the integration $d\Omega_{34}^{**}$ in the rest frame of p_{34}, then we integrate out s_{34} and θ_{234}^* in the rest frame of p_{234}, the last variable s_{234} is integrated out in Υ rest frame. Since $|\vec{p}_1|$ only depends on s_{234}, the J/ψ momentum spectrum could be easily obtained by replacing ds_{234} with $[(ds_{234})/(d|\vec{p}_1|)]d|\vec{p}_1|$. The phase-space integrations for the total rate and J/ψ momentum spectrum are calculated numerically.

[1] N. Brambilla *et al.* (Quarkonium Working Group), arXiv: hep-ph/0412158.
[2] G. T. Bodwin, E. Braaten, and G. P. Lepage, Phys. Rev. D **51**, 1125 (1995); **55**, 5853(E) (1997).
[3] F. Abe *et al.* (CDF Collaboration), Phys. Rev. Lett. **69**, 3704 (1992).
[4] E. Braaten and S. Fleming, Phys. Rev. Lett. **74**, 3327 (1995).
[5] A. A. Affolder *et al.* (CDF Collaboration), Phys. Rev. Lett. **85**, 2886 (2000).
[6] B. Gong, X. Q. Li, and J. X. Wang, Phys. Lett. B **673**, 197 (2009).
[7] J. M. Campbell, F. Maltoni, and F. Tramontano, Phys. Rev. Lett. **98**, 252002 (2007); B. Gong and J. X. Wang, Phys. Rev. Lett. **100**, 232001 (2008); Phys. Rev. D **78**, 074011 (2008).
[8] P. Artoisenet, J. M. Campbell, J. P. Lansberg, F. Maltoni, and F. Tramontano, Phys. Rev. Lett. **101**, 152001 (2008).
[9] D. E. Acosta *et al.* (CDF Collaboration), Phys. Rev. Lett. **88**, 161802 (2002).
[10] V. M. Abazov *et al.* (D0 Collaboration), Phys. Rev. Lett. **101**, 182004 (2008).
[11] E. Braaten and Y. Q. Chen, Phys. Rev. Lett. **76**, 730 (1996); F. Yuan, C. F. Qiao, and K. T. Chao, Phys. Rev. D **56**, 321 (1997).
[12] B. Aubert *et al.* (*BABAR* Collaboration), Phys. Rev. Lett. **87**, 162002 (2001).
[13] K. Abe *et al.* (BELLE Collaboration), Phys. Rev. Lett. **88**, 052001 (2002).
[14] S. Fleming, A. K. Leibovich, and T. Mehen, Phys. Rev. D **68**, 094011 (2003).
[15] K. Abe *et al.* (Belle Collaboration), Phys. Rev. Lett. **89**, 142001 (2002); P. Pakhlov *et al.* (Belle Collaboration), Phys. Rev. D **79**, 071101 (2009).
[16] Y. J. Zhang and K. T. Chao, Phys. Rev. Lett. **98**, 092003 (2007).
[17] B. Gong and J. X. Wang, Phys. Rev. D **80**, 054015 (2009).
[18] Y. Q. Ma, Y. J. Zhang, and K. T. Chao, Phys. Rev. Lett. **102**, 162002 (2009).
[19] B. Gong and J. X. Wang, Phys. Rev. Lett. **102**, 162003 (2009).
[20] K. M. Cheung, W. Y. Keung, and T. C. Yuan, Phys. Rev. D **54**, 929 (1996).
[21] M. Napsuciale, Phys. Rev. D **57**, 5711 (1998).
[22] R. Fulton *et al.* (CLEO Collaboration), Phys. Lett. B **224**, 445 (1989).
[23] H. Albrecht *et al.* (ARGUS Collaboration), Z. Phys. C **55**, 25 (1992).
[24] R. A. Briere *et al.* (CLEO Collaboration), Phys. Rev. D **70**, 072001 (2004).
[25] H. D. Trottier, Phys. Lett. B **320**, 145 (1994).
[26] S. Y. Li, Q. B. Xie, and Q. Wang, Phys. Lett. B **482**, 65 (2000); W. Han and S. Y. Li, Phys. Rev. D **74**, 117502 (2006).
[27] H. Fritzsch and K. H. Streng, Phys. Lett. **77B**, 299 (1978).
[28] I. I. Y. Bigi and S. Nussinov, Phys. Lett. **82B**, 281 (1979).
[29] J.-X. Wang, Nucl. Instrum. Methods Phys. Res., Sect. A **534**, 241 (2004).
[30] E. J. Eichten and C. Quigg, Phys. Rev. D **52**, 1726 (1995).
[31] C. Amsler *et al.* (Particle Data Group), Phys. Lett. B **667**, 1 (2008).
[32] Z. H. Lin and G. h. Zhu, Phys. Lett. B **597**, 382 (2004).
[33] G. Hao, Y. Jia, C. F. Qiao, and P. Sun, J. High Energy Phys. 02 (2007) 057; B. Gong, Y. Jia, and J. X. Wang, Phys. Lett. B **670**, 350 (2009).
[34] J. H. Kuhn, J. Kaplan, and E. G. O. Safiani, Nucl. Phys. **B157**, 125 (1979); B. Guberina, J. H. Kuhn, R. D. Peccei, and R. Ruckl, Nucl. Phys. **B174**, 317 (1980).
[35] P. L. Cho and A. K. Leibovich, Phys. Rev. D **53**, 150 (1996); **53**, 6203 (1996); P. Ko, J. Lee, and H. S. Song, Phys. Rev. D **54**, 4312 (1996); **60**, 119902(E) (1999).